

# Theoretical Analysis and Performance of OFDM Signals in Nonlinear Fading Channels

Paolo Banelli, *Member, IEEE*

**Abstract**—This paper presents an analytical framework to calculate the average symbol-error rate (SER) of uncoded orthogonal frequency-division multiplexing (OFDM) systems in realistic scenarios impaired by transmitter nonlinearity and frequency-selective fading channels. The results are applicable to cyclically extended OFDM signals characterized by a high number of carriers, which can be modeled as complex Gaussian processes. To avoid intercarrier interference, we also assume that the symbol duration is shorter than the channel coherence time. We derive analytical SER results in Rayleigh and Rice frequency-selective fading channels, for both the nonlinear amplification and the ideal predistortion case. Simulations results demonstrate the validity of the analytical results.

**Index Terms**—Communication system nonlinearity, fading channels, nonlinear distortions, orthogonal frequency-division multiplexing (OFDM), predistortion.

## I. INTRODUCTION

ORTHOGONAL frequency-division multiplexing (OFDM) is widely employed in wireless communication systems like digital audio broadcasting (DAB) [1], digital video broadcasting-terrestrial (DVB-T) [2], and HYPERLAN/2 [3] for wireless local-area network (WLAN). The mixture of code-division multiple access (CDMA) and OFDM is considered to be a good candidate for future generation mobile wireless systems [4]. Wireless communications are generally subject to severe multipath fading channels that can seriously degrade the system performance. Counteracting the frequency selectivity of multipath channels by multiplexing information on different orthogonal carriers is the key to the OFDM success. Indeed, if a cyclic prefix is inserted between successive OFDM symbols, the overall system can be viewed as composed of  $N$  parallel frequency flat channels [4]–[6]. In modern communication systems, which take advantage of the fast Fourier transform (FFT) processing to realize an OFDM modem, the channel induced distortions can then easily be compensated at the receiver side by a complex multiplication of each FFT output. An OFDM signal is generally characterized by the sum of a high number of carriers. This causes a highly variable envelope, which makes the technique sensitive to nonlinear distortions introduced by real hardware (power amplifiers, analog-to-digital–digital-to-analog (A/D-D/A) converters, etc.). A complex baseband OFDM signal, with a

high number of carriers, can be modeled as a complex Gaussian process due to the central limit theorem [8] and, consequently, the distortions introduced by nonlinear amplifiers can be modeled and computed by means of a complex extension [7], [10] of the Bussgang theorem [8]. Analytical results for both the nonlinearity output power spectral density (PSD) and the symbol-error rate (SER) performance in additive white Gaussian noise (AWGN) channels are carried out in [9]–[11]. The aim of this work is to extend the analytical results obtained in [9] to more realistic wireless scenarios, where the nonlinear amplification and the frequency-selective fading jointly affect the SER performance. The typical OFDM system architecture, the nonlinear amplifier model and the fading channel model are analyzed in Section II. To characterize the nonlinear distortion phenomena, a brief summary of the results obtained in [9] is also given in Section II. The analytical results for the system under consideration are derived in Section III and they will be compared with the simulation results in Section IV. Finally, some conclusions are drawn in Section V.

## II. SYSTEM DESCRIPTION

### A. OFDM System Architecture

A general architecture of an OFDM system is shown in Fig. 1. The complex baseband samples of an OFDM signal (without the guard time interval) transmitted during an OFDM block duration  $T_b = NT_c$ , are expressed by [6], [12]

$$z_m[k] = \sum_{n=0}^{N-1} a_m[n] e^{j\omega_n k T_c}, \quad k = 0, \dots, N-1 \quad (1)$$

where  $a_m[n]$  represents the complex information symbol transmitted during the  $m$ th OFDM block on the  $n$ th subcarrier and  $\omega_n = 2\pi n/T_b$  is the angular frequency of the  $n$ th subcarrier.

The symbols  $a_m[n]$  are the results of mapping bits on a complex constellation [e.g., M-quadrature amplitude modulation (QAM), M-differential phase-shift keying (DPSK), M-phase-shift keying (PSK)] imposed by the application (e.g., DAB, DVB-T, IEEE 802.11, etc.). The time continuous complex signal  $z(t) = r(t) \exp[j\theta(t)]$ , which is obtained from  $z_m[k]$  after the parallel to serial (P/S) conversion and the D/A conversions, is transmitted by a power amplifier whose instantaneous nonlinear distortions are usually modeled by means of a complex nonlinear distorting function  $f(r) = g(r) \cdot e^{j\phi(r)}$ , which only depends on the envelope  $r(t)$  of the input signal  $z(t)$  and where  $g(r)$  and  $\phi(r)$  are the AM-AM and AM-PM distorting curves, respectively [13], [14]. Thus, the output signal  $z_d(t)$  can be expressed by

$$z_d(t) = f[r(t)] \cdot e^{j\theta(t)} = g[r(t)] \cdot e^{j\{\theta(t) + \phi[r(t)]\}}. \quad (2)$$

Manuscript received March 7, 2001; revised April 19, 2002; accepted April 19, 2002. The editor coordinating the review of this paper and approving it for publication is K. Wilson.

The author is with the Department of Electronic and Information Engineering (DIEI), University of Perugia, 06128 Perugia, Italy (e-mail: banelli@diei.unipg.it).

Digital Object Identifier 10.1109/TWC.2003.808969

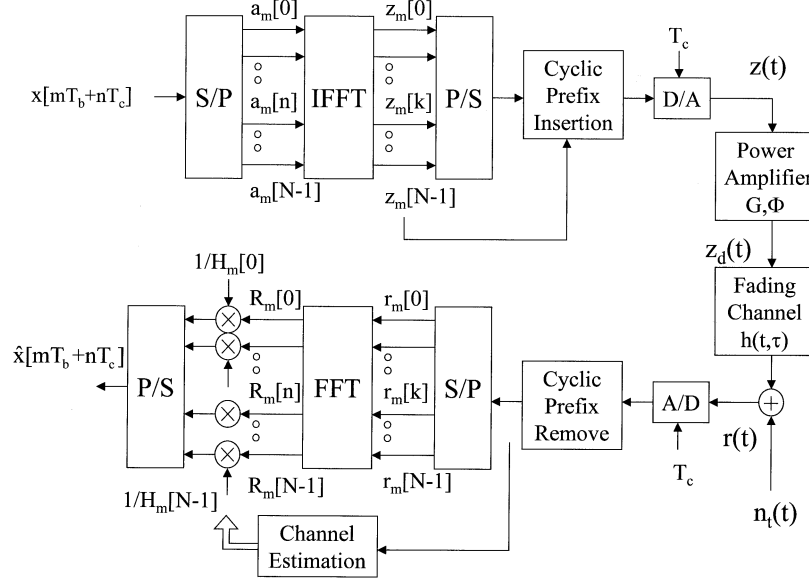


Fig. 1. OFDM system architecture.

The extension of the Busgang theorem to complex Gaussian inputs [7], [10], allows expressing the nonlinear output  $z_d(t)$  as the sum of a complex-scaled useful input replica and an uncorrelated nonlinear distortion noise  $n_d(t)$ , as expressed by

$$z_d(t) = z_u(t) + n_d(t) = \alpha \cdot z(t) + n_d(t) \quad (3)$$

where  $\alpha$  is time invariant for stationary input processes. Although the OFDM signal  $z(t)$  is not stationary, it has been shown in [10] that an OFDM signal guarantees  $\alpha$  to be time invariant if it is obtained by a rectangular pulse shaping of the IFFT outputs in the D/A converter of Fig. 1 or by a band-limited pulse shaping in the frequency range  $[-1/(2T_c); 1/2T_c]$ . This is assumed in the current paper.

For a slowly varying channel, with a coherence time longer than the OFDM block duration  $T'_b = T_b + \Delta T_b$ , where  $\Delta T_b$  is the guard time duration, the channel is assumed to be time invariant for each transmitted OFDM block. The choice to use the guard-time interval to introduce a cyclic extension of the OFDM block is generally adopted in order to reduce the equalizer complexity at the receiver side. Indeed, for the  $m$ th OFDM block, each FFT output at the receiver side is expressed by [4], [5]

$$R_m[n] = \sum_{k=0}^{N-1} r_m[k] e^{-j(2\pi/N)kn} \quad (4)$$

where  $r(t) = \int_{-\infty}^{+\infty} h(t, \tau) x(t - \tau) d\tau$  is the signal received through the time-varying channel  $h(t, \tau)$ ,  $r_m[k] = r(mT'_b + \Delta kT_c)$  is the sampled receiver input after the cyclic extension removal and it is straightforward from (1) to derive that [4], [12]

$$R_m[n] = \alpha \cdot H_m[n] \cdot a_m[n] + H_m[n] \cdot N_{d,m}[n] + N_{t,m}[n] \quad (5)$$

$n = 0, \dots, N - 1$

where the generic signal “ $X_m[n]$ ” represents the FFT output corresponding to the signal “ $x_m[k]$ ” during the  $m$ th OFDM block,  $x_m[k] = x(mT'_b + kT_c)$ ,  $H(t, f) =$

$\int_{-\infty}^{+\infty} h(t, \tau) e^{-j2\pi f\tau} d\tau$  is the time varying channel transfer function,  $H_m[n] = H(mT'_b, n/T_b)$  and  $1/T_b$  is the frequency separation between each subcarrier.

Expression (5) outlines that the symbol received on each subcarrier is a complex distorted replica of the transmitted one, corrupted by two noise terms. The  $H_m[n]N_{d,m}[n]$  contribution represents the nonlinear distortion noise filtered by the channel, while the  $N_{t,m}[n]$  contribution represents the thermal Gaussian noise at the receiver side. The nonlinear distortion noise  $N_{d,m}[n]$  can be modeled by a zero-mean complex Gaussian random variable (characterized by uncorrelated real and imaginary components with equal power  $(\sigma_{NL}^2)_n$ ) if the power input backoff  $\gamma$  is not too high (i.e., for  $\gamma \leq 9$  dB for DVB-T systems that employ thousands of carriers, or for a lower  $\gamma$  if the number of carriers decreases). The Gaussian nature of the nonlinear distortion noise can be explained by the fact that  $N_{d,m}[n]$  is obtained by a linear combination, through the FFT coefficients, of the distortion noise introduced in the time domain on a block of samples  $r_m[k]$  [9], thus generating a Gaussian-like clustering of the constellation points transmitted on each carrier [19]. The Gaussian assumption of  $N_{d,m}[n]$  will be the basis for the performance analysis in Section III.

### B. Channel Model

In order to rigorously motivate the analytical performance evaluation, we need to statistically characterize the channel coefficients  $H_m[n]$ , which by (5) impairs the transmission over each subcarrier. A popular and general representation of the function  $h(t, \tau)$  in (4) is [15]

$$h(t, \tau) = \sum_{i=0}^{L-1} \beta_i(t) \delta[\tau - \tau_i(t)] \quad (6)$$

where a multipath fading channel is modeled as the sum of  $L$  frequency flat channels. In nonlinear-of-sight (NLOS) conditions the  $\beta_i(t)$  coefficients are generally modeled as zero-mean complex Gaussian processes, whereas in LOS conditions at least one coefficient is a nonzero-mean Gaussian process. The propagation

delay  $\tau_i(t)$  associated to each path can also be considered time invariant like for the COST-207 channel [16].

Under these hypotheses, the channel coefficients  $H_m[n]$  are expressed by

$$H_m[n] = \sum_{i=0}^{L-1} \beta_i[m] e^{-j2\pi\tau_i n/T_b}. \quad (7)$$

Clearly,  $H_m[n]$  is a complex Gaussian random variable because it is a linear combination of Gaussian random variables and it is easy to proof [12] that, if  $\beta_i[m] = \beta_{Ri}[m] + j\beta_{Ii}[m]$  has uncorrelated real and imaginary components with the same variance  $\sigma_{\beta_i}^2$ , then  $H_m[n]$  has uncorrelated components too and its envelope  $\rho_{H_m}[n] = |H_m[n]|$  is characterized by a Rice probability density function (pdf). Specifically, if the channel has a single LOS path, then the Rice pdf of  $\rho_{H_m}[n]$  is independent of the block index  $m$  and the carrier index  $n$  and it is expressed by

$$\begin{aligned} p_{\rho_H}(\rho_H) &= \frac{\rho_H}{\sigma_H^2} e^{-(\rho_H^2 + A_H^2)/2\sigma_H^2} I_0\left(\frac{A_H \rho_H}{\sigma_H^2}\right) \\ \sigma_H^2 &= \sum_{i=0}^{L-1} \sigma_{\beta_i}^2 \\ A_H &= \sqrt{\bar{H}_R^2 + \bar{H}_I^2} = \sqrt{\bar{\beta}_{oR}^2 + \bar{\beta}_{oI}^2} \end{aligned} \quad (8)$$

where  $(\bar{H}_R + j\bar{H}_I)$  is the mean-value of the channel transfer function and  $(\bar{\beta}_{oR} + j\bar{\beta}_{oI})$  is the mean-value of the LOS coefficient  $\beta_o$ . The envelope  $\rho_H$  is still Rice distributed even with multiple LOS paths, but the Rice pdf will only be time invariant if the delays  $\tau_i$  associated to the LOS paths themselves are time invariant. The previous hypotheses, which are encountered in most realistic scenarios, greatly simplify the analytical evaluation of the system performance and allow averaging the SER performance over a single pdf of the signal-to-noise ratio (SNR) rather than over a number of pdfs equal to the number of subcarriers [see (25)–(28)].

### C. Nonlinear Distortion PSD

The PSD evaluation at the nonlinearity output is not the main subject of this paper and the interested reader is referred to [9]. Anyway, some concepts developed in [9] that are necessary to evaluate the SER performance are briefly summarized in this paragraph to assist the reader. The analytical computation of the output PSD and its separation in useful and nonlinear noise components by means of (3) and (9), allow to exactly compute the system performance. Indeed, only the in-band frequency components of the nonlinear distortion noise have to be taken into account to precisely compute the SER performance. This is different from [10], where all the nonlinear noise power was considered in AWGN channels.

The PSD of the nonlinear output  $z_d(t)$  in (3) can be expressed by

$$\begin{aligned} S_{z_d z_d}(\nu) &= |\alpha|^2 S_{zz}(\nu) + S_{n_d n_d}(\nu) \\ &= \frac{c_0}{(2\sigma^2)} S_{zz}(\nu) \\ &\quad + \sum_{n_o=1}^{\infty} \frac{c_{n_o}}{(2\sigma^2)^{2n_o+1}} [S_{ss}(\nu) \otimes_1 \cdots \otimes_{2n_o+1} S_{ss}(\nu)] \end{aligned} \quad (9)$$

where the  $n_o$ th term in the series represents the  $(2n_o + 1)$ th auto convolution of the input PSD  $S_{zz}(\nu)$ .

The coefficients  $c_{n_o}$  are expressed by [9]

$$\begin{aligned} c_{n_o} &= \frac{1}{2\sigma^2} \frac{1}{n_o + 1} \\ &\quad \cdot \left\| \int_{D(r)} f(r) \cdot \frac{r^2}{\sigma^2} \cdot e^{-(r^2/2\sigma^2)} \cdot L_{n_o}^{(1)}\left(\frac{r^2}{2\sigma^2}\right) dr \right\|^2 \end{aligned} \quad (10)$$

where  $D(r) = \{r : 0 \leq r \leq \infty\}$  is the integration domain and  $L_{n_o}^{(1)}(x)$  is the Laguerre polynomial of the first kind and  $n_o$ th order. The coefficients  $c_{n_o}$  depend not only on the nonlinear distorting function  $f(r)$ , as explicitly shown by (10), but also on the input-backoff  $\gamma$  that represents the ratio between the input saturation power of the nonlinearity  $f(r)$  and the mean power of the input signal  $s(t)$ .

Closed form expressions of the coefficients  $c_{n_o}$  are derived in [9], either when the complex nonlinearity  $f(r)$  represents the amplifier AM/AM and AM/PM curves and it is expressed by a Bessel series expansion

$$\begin{aligned} f(r) &= \sum_{m_o=1}^L b_{m_o} J_1\left(\frac{(2m_o - 1)\pi}{R_{\max}} \cdot r\right) \\ &= \sum_{m_o=1}^L b_{m_o} J_1\left(\beta(m_o, \gamma) \frac{\sqrt{\gamma}}{A} r\right) \end{aligned} \quad (11)$$

or when  $f(r)$  represents the ideally predistorted amplifier as expressed by

$$f(r) = \begin{cases} r, & r \leq A \\ A, & r > A \end{cases} \quad (12)$$

where  $R_{\max}$  and  $A$  are the normalization coefficients [14].

### III. OFDM PERFORMANCE IN NONLINEAR FADING CHANNELS

This section derives the analytical SER performance of OFDM systems in nonlinear frequency-selective fading channels, by extending the analysis for the linear case. The symbol  $R_m[n]$  received during the  $m$ th OFDM block on the  $n$ th subcarrier is expressed by (5). It should be clear from Section II-B that the transmission of the information symbols  $a_m[n]$  over each subcarrier is impaired by a flat Rice fading channel as expressed by

$$R_m[n] = \eta_m[n] a_m[n] + N_m[n] \quad (13)$$

with a fading coefficient  $\eta_m[n] = \alpha H_m[n]$  and an additive noise term  $N_m[n] = H_m[n] N_{d,m}[n] + N_{t,m}[n]$ . The envelope  $\rho_{\eta} = |\eta_m[n]|$  of the coefficient  $\eta_m[n]$  is Rice distributed because it is obtained by scaling the Rice random variable  $\rho_{H_m}[n] = |H_m[n]|$  by the quantity  $|\alpha|$ . Thus, each OFDM subchannel is modeled as a classical Rice flat fading channel where, in the nonlinear scenario, the fading process influences also the noise term. The amplifier contribution  $\alpha$  and the channel contribution  $H_m[n]$  to the distortion of the useful signal will be indistinguishable to any channel estimation technique. Consequently, with perfect channel state information at

the receiver side, the estimated symbol  $\hat{a}_m[n]$  obtained by zero forcing (ZF) equalization is given by

$$\hat{a}_m[n] = \frac{R_m[n]}{\alpha \cdot H_m[n]} = a_m[n] + \frac{N_{d,m}[n]}{\alpha} + \frac{N_{t,m}[n]}{\alpha \cdot H_m[n]}. \quad (14)$$

It is well-known that in a single-tap scenario the minimum mean square error (MMSE) equalizer is given by

$$\tilde{a}_m[n] = \frac{\alpha^* H_m^*[n]}{|\alpha H_m[n]|^2 + \frac{\sigma_t^2}{E_a}} R_m[n] = \frac{|\alpha H_m[n]|^2}{|\alpha H_m[n]|^2 + \frac{\sigma_t^2}{E_a}} \hat{a}_m[n] \quad (15)$$

where  $E_a = E\{|a_m|^2\}$  is the constellation mean power and  $\sigma_t^2 = E\{|N_t|^2\}$  the thermal noise power.

The MMSE equalizer is clearly equivalent to a scaled version of the ZF and consequently it performs as the ZF if the decision thresholds after the equalization are accordingly scaled. Thus, there is no reason to use an MMSE equalizer and in the sequel we will consider the ZF expression (14), which leads to manageable analytical expressions for the SER.

Without the nonlinear distortion, (14) reduces to (16) which resembles the classical linear flat fade phenomenon

$$\hat{a}_m[n] = a_m[n] + \frac{N_{t,m}[n]}{H_m[n]}. \quad (16)$$

It is well-known that the mean SER performance in such an environment can be obtained by [15], [17]

$$(\text{SER})_n = \int_{-\infty}^{+\infty} P_{\text{err}}(\chi_n) p(\chi_n) d\chi_n \quad (17)$$

where  $\chi_n$  is the channel affected SNR as expressed by

$$\chi_n = |H_m[n]|^2 \frac{E_a}{\sigma_t^2} = |\rho_H|^2 \frac{E_a}{\sigma_t^2} \quad (18)$$

$p(\chi_n)$  is the corresponding pdf and  $P_{\text{err}}(\chi)$  is the error probability, which depends on the  $a_m[n]$  mapping. It is known that  $p(\chi_n)$ , which is independent of the  $m$ th block, is either an exponential or a chi-squared pdf with two degrees of freedom, if  $\rho_m[n] = |H_m[n]|$  is either a Rayleigh or a Rice random variable, respectively. Specifically,  $p(\chi_n)$  is given by

$$p(\chi_n) = \begin{cases} \frac{1}{\chi_o} \exp\left(-\frac{\chi_n}{\chi_o}\right), & \chi_n \geq 0 \\ 0, & \chi_n < 0 \end{cases} \quad (19)$$

or see (20), shown at the bottom of the page.

The parameter  $\chi_o$ , which represents the mean SNR, is independent of the  $n$ th subcarrier if the channel is characterized by a single LOS (as assumed in the following) and is expressed by

$$\chi_o = \begin{cases} 2\sigma_H^2 \cdot \frac{E_a}{\sigma_t^2}, & |H| \text{ Rayleigh} \\ (1 + Q^2) 2\sigma_H^2 \cdot \frac{E_a}{\sigma_t^2}, & |H| \text{ Rice} \end{cases} \quad (21)$$

where  $Q^2 = A_H^2/2\sigma_H^2$  is the power ratio between the LOS and the NLOS contributes.

Expressions (16) and (17) state the well known fact that the SER performance for each  $n$ th subcarrier of an OFDM system,

in a frequency-selective fading channel, is the same SER of a single carrier system in a frequency-flat fading channel.

In the nonlinear fading scenario, the SNR for a given  $H_m[n]$  becomes

$$\begin{aligned} (\chi_{\text{TOT}})_n &= \frac{E\{|a_m|^2\}}{\frac{E\{|N_{d,m}[n]|^2\}}{|\alpha|^2} + \frac{E\{|N_{t,m}[n]|^2\}}{|\alpha|^2 \cdot |H_m[n]|^2}} \\ &= \frac{E_a}{\frac{(\sigma_d^2)_n}{|\alpha|^2} + \frac{\sigma_t^2}{|\alpha|^2 \cdot |H_m[n]|^2}}. \end{aligned} \quad (22)$$

The SNR on the  $n$ th subcarrier  $(\chi_{\text{TOT}})_n$  in (22) can be expressed as a function of the SNR  $\chi_n$  in linear fading conditions

$$(\chi_{\text{TOT}})_n = \left[ \frac{1}{(\chi_{\text{NL}})_n} + \frac{1}{|\alpha|^2 \cdot \chi_n} \right]^{-1} \quad (23)$$

where  $(\chi_{\text{NL}})_n$  is the nonfaded SNR at the nonlinearity output, or equivalently, the SNR at the receiver side in absence of thermal noise, on the  $n$ th subcarrier. From [9], we know that

$$(\chi_{\text{NL}})_n = \frac{c_o^2}{2\sigma^2} \cdot \frac{S_{zz}\left(\frac{n}{T_b}\right)}{S_{n_d n_d}\left(\frac{n}{T_b}\right)} \quad (24)$$

where  $S_{zz}(\nu)$  and  $S_{n_d n_d}(\nu)$  are used to denote the PSD of the input signal  $z(t)$  and the PSD of the distortion noise signal  $n_d(t)$ , respectively [see (3) and (9)]. We want to point out that  $(\chi_{\text{NL}})_n$  depends on the nonlinearity  $f(r)$  as can be seen from (9) and (10).

Modifying (17) by (23) the uncoded mean SER for the  $n$ th subcarrier results computable by

$$(\text{SER})_n = \int_{-\infty}^{+\infty} P_{\text{err}} \left[ \left( \frac{1}{(\chi_{\text{NL}})_n} + \frac{1}{|\alpha|^2 \chi_n} \right)^{-1} \right] p(\chi_n) d\chi_n. \quad (25)$$

The expression of  $P_{\text{err}}(\cdot)$  for an AWGN channel is still used because the total noise  $N_m[n]$  at the receiver side is the sum of the two independent Gaussian contributions (i.e.,  $N_{t,m}[n]$  and  $H_m[n]N_{d,m}[n]$ ), which represent the thermal and the channel-scaled nonlinear noise, respectively. Alternatively, the SER can be computed by the following:

$$(\text{SER})_n = \int_{-\infty}^{+\infty} P_{\text{err}}[(\chi_{\text{TOT}})_n] p[(\chi_{\text{TOT}})_n] d(\chi_{\text{TOT}})_n \quad (26)$$

where  $p[(\chi_{\text{TOT}})_n]$  is obtained from  $p(\chi_n)$  in Appendix A [8]. Clearly, both (25) and (26) reduce to (17) when nonlinear distortions are avoided, i.e., when  $(\chi_{\text{NL}})_n = \infty$  and  $\alpha = 1$ . The mean SER for the OFDM system is simply obtained by averaging the mean SERs of all the subcarriers, as expressed by

$$\overline{\text{SER}} \approx \frac{1}{N_a} \sum_{n=1}^{N_a} (\text{SER})_n \quad (27)$$

$$p(\chi_n) = \begin{cases} \frac{1+Q^2}{\chi_o} e^{-Q^2} \exp\left[-(1+Q^2) \frac{\chi_n}{\chi_o}\right] \cdot I_0\left(2Q\sqrt{(1+Q^2) \frac{\chi_n}{\chi_o}}\right), & \chi_n \geq 0 \\ 0, & \chi_n < 0 \end{cases} \quad (20)$$

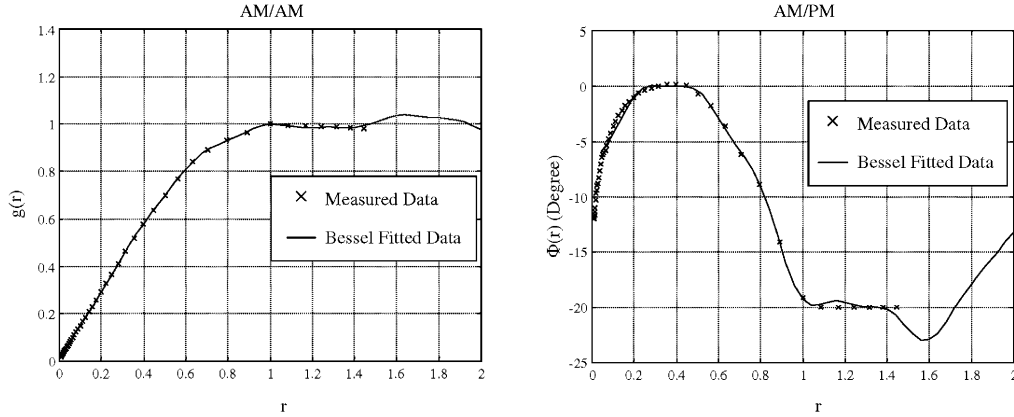


Fig. 2. Measured AM/AM and AM/PM: fitting by Bessel series expansion.

where  $N_a$  represents the number of active carriers used to transmit information within the total number  $N$  of carriers. In order to reduce the computing time involved in the numerical evaluation of (25) or (26) for all the  $N_a$  subcarriers, the SER can be approximated by

$$\overline{\text{SER}} \approx \int_{-\infty}^{+\infty} P_{\text{err}} \left[ \left( \frac{1}{\bar{\chi}_{NL}} + \frac{1}{|\alpha|^2 \chi} \right)^{-1} \right] p(\chi) d\chi \quad (28)$$

where

$$\bar{\chi}_{NL} = \frac{1}{N_a} \sum_{n=1}^{N_a} (\chi_{NL})_n \quad (29)$$

is the mean nonlinear SNR for all the  $N_a$  active subcarriers and  $\chi = \chi_n$  for any  $n$  in a single LOS scenario.

The use of (28) and (29) instead of (25) and (27) produces a very low inaccuracy in the evaluation of the SER performance of the OFDM system because the nonlinear SNR  $(\chi_{NL})_n$  expressed by (24) is quite the same for most of the  $N_a$  active carriers. Indeed, the PSD  $S_{zz}(n/T_b)$  of the useful OFDM signal is usually constant for each subcarrier while the nonlinear distortion noise  $n_d(t)$  is characterized by a quasi-constant PSD inside the useful OFDM bandwidth, with monotonically decreasing values starting from the band center up to the band edges [9].

Generally, forward error correction techniques are employed to mitigate the SER degradation introduced by frequency-selective channels. The relationship between the uncoded SER, which can be estimated at the input of the channel decoder and the coded SER at the output, depends not only on the selected coding technique, but also on the channel that generates the errors at the input of the receiver's decoder. The DVB-T system makes use of a complex channel coding scheme that exploits a Reed–Solomon block code concatenated to a convolutional code, as well as time and frequency interleavers (see [2] for further details). Anyway, the evaluation of the coded performance of an OFDM system in nonlinear fading channels is beyond the scope of the present paper and it would require a dedicated work. We refer the interested reader to [21]–[23] for coded performance in a linear scenario.

#### IV. SIMULATION RESULTS

In this section, we show a performance comparison between analytical results and computer simulations as a verification of the analytical approach. The DVB-T system, with uniform M-QAM constellations, has been chosen as a reference although the conclusions are extensible to any OFDM system as long as the FFT size  $N$  is large enough to satisfy the Gaussian signal assumption, the cyclic extension of the OFDM block is used to eliminate ISI and the OFDM block duration is lower than the channel coherence time.

The DVB-T signal in the 2K-mode operating condition [2] is formed by 2048-length blocks ( $N = 2048$ ) characterized by a duration  $T_b = 224 \mu\text{s}$  (without the guard time  $\Delta T_b$ ). We have over sampled by four each DVB-T block in the time domain in order to obtain an adequate signal representation in a nonlinear environment. The interpolated signal has been successively distorted during the simulations by the curves (11) and (12), which represent the AM/AM-AM/PM distorting amplifier and the ideally predistorted amplifier, respectively. The values of the coefficients  $b_{m_0}$ ,  $R_{\text{max}}$  and  $A$ , used in (11) to represent the distorting amplifier of Fig. 2, have been obtained by fitting the measurement carried out on a real DVB-T amplifier and they are detailed in Appendix B.

The DVB-T standard [2] maps the information bits on a M-QAM constellation with size  $M$ , which can be equal to 4, 16, or 64 depending on the applications and scenarios. Consequently, the expression of the symbol error probability  $P_{\text{err}}(\cdot)$  that must be used in (17), (25), (26), or (28) to calculate the mean SER for each subcarrier [15] is given by

$$P_{\text{err}}(\chi) = 1 - \left[ 1 - 2 \left( 1 - \frac{1}{\sqrt{M}} \right) Q_o \left( \sqrt{\frac{3}{M-1} \chi} \right) \right]^2 \quad (30)$$

where  $\chi$  is the average SNR per symbol and  $Q_o(x) = 0.5 \cdot \text{erfc}(x/\sqrt{2})$ .

It is important to outline that the SNR at the receiver for the  $n$ th subcarrier, after the FFT processing, is generally defined as the power ratio between the received signal  $R[k]$  and the thermal noise  $N_t[k]$ . This SNR will be termed “apparent” and denoted as  $\chi_{\text{App}}$  because it is not the SNR that establishes the performance. It is, however, the measurable SNR at the receiver and,

TABLE I  
 2K-DVBT CARRIERS TYPE

CARRIERS TYPE	Symbol	Number	Relative Mean Power
Data	$N_{Data}$	1512	1
Continuous	$N_{Cont}$	45	16/9
Scattered	$N_{Scatt}$	131	16/9
TPS	$N_{TPS}$	17	1
Guard Band (Switched Off)	$N_{Guard}$	343	0
Active	$N_{Act}$	1705	1.0802
Total	$N_{Tot}$	2048	0.89935

thus, this is the SNR the SER performances are plotted against. On the contrary, the SNR  $\chi_{TOT}$  in (23) is the effective SNR that establishes the performance at the receiver in presence of nonlinear distortions, as expressed by (25) and (26). Indeed, it represents the power ratio between the useful signal and the total noise at the receiver side, after the FFT processing. It is easy to show that the two SNRs are related one with another by

$$\frac{1}{\chi_{TOT}} = \frac{2\sigma_H^2 \cdot \sigma_{NL}^2 + \sigma_t^2}{2\sigma_H^2 \cdot |\alpha|^2 E_a} = \frac{1}{\chi_{NL}} \left[ 1 + \frac{1}{\chi_{APP}} \right] + \frac{1}{\chi_{APP}}. \quad (31)$$

Moreover, it is important to note that the 2048 subcarriers, available in the 2k-mode of the DVB-T system, are not all used to transmit information. Some of them are switched off to implement a guard band between adjacent channels, while other carriers, named ‘‘pilot carriers,’’ are used to deliver system configuration parameters, synchronization information and channel sounding signals in order to help the receiver in the demodulation process. The 2048 carriers are divided as detailed in Table I. Note that different types of carriers are transmitted with different powers. As a consequence, a normalization factor must be introduced between the overall SNR (generally measured) and the effective SNR responsible for the system performance on the data subcarriers, which is the one we use in the SER performance analysis [see (25), (26), and (30)].

The SER performance can be exactly calculated either by the expressions (26)–(27) or (28)–(29) and they can be compared with the simulation results by using

$$\chi_{TOT} = \frac{\left(\frac{16}{9}\right) \cdot (N_{Cont} + N_{Scatt}) + (N_{Data} + N_{TPS})}{(N_{Cont} + N_{Scatt} + N_{TPS} + N_{Data})} \cdot \chi_{Data} \quad (32)$$

which expresses the relationship between the overall SNR  $\chi_{TOT}$  and the SNR  $\chi_{Data}$  of the data carriers. By substituting the values shown in Table I, the expression (32) becomes in decibels

$$(\chi_{TOT})_{dB} \approx (\chi_{Data})_{dB} + 0.34 \text{ dB} \quad (33)$$

while the relation between SNR and the  $E_b/N_o$  parameter is expressed by

$$(\chi)_{dB} = \left(\frac{E_b}{N_o}\right)_{dB} + (n_{bit})_{dB} \quad (34)$$

where  $n_{bit} = \log_2(M)$  is the number of bits per symbol transmitted by the M-QAM mapping.

The simulations have been performed with perfect channel inversion and perfect intersymbol interference (ISI) elimination by adequate cyclic extension, as supposed in the theoretical analysis.

The channels used in the simulations are standardized by COST 207 [16] and they are compliant with the general channel model of Section II-B. The COST 207 model encompasses four different scenarios (‘‘hilly terrain,’’ ‘‘bad urban,’’ ‘‘typical urban,’’ and ‘‘rural area’’) each of which is characterized by a typical delay spread and power delay profile. Each channel model is further characterized by the sum of different flat Rayleigh fading channels corresponding to different path delays, except for the first path that is modeled by a flat Rice fading channel in order to take possible LOS condition into account. The parameter  $Q$  of (20) and (21), which defines the power ratio between the signal received over the LOS path and the ones that propagate over the NLOS paths, is one of the parameters that have been considered to plot the SER performance. The output backoff (*obo*) is another important parameter. It is the key parameter for a meaningful comparison between the predistorted and the nonpredistorted scenario. The *obo* is defined as the ratio between the maximum and the mean amplifier output power. It generally depends on both the input backoff  $\gamma$  and the nonlinear distortion  $f(r)$ . For the ideal predistortion of (12), the *obo* is given by [9]

$$obo = \gamma \cdot (1 - e^{-\gamma})^{-1} \quad (35)$$

Fig. 3 shows a good agreement between analytical and simulation results in different scenarios, ranging from nonlinear amplification to ideal predistortion, with different ratio  $Q$  between the direct and the scattered paths, different *obo* and different modulation size  $M$ . All the theoretical results are derived by means of (28), which means that (28) is a good approximation of the exact uncoded SER performance expressed by (27). Other analytical results are shown in Fig. 5(a)–(d). All these figures show the uncoded SER performance. In practice, the DVB-T system includes a punctured concatenated channel code to improve the SER performance. The DVB-T standard requires a BER equal to  $2 \cdot 10^{-4}$  ( $SER \approx n_{bit} \cdot BER \approx 4 \cdot 10^{-4} / 8 \cdot 10^{-4} / 1.2 \cdot 10^{-3}$  for 4/16/64—QAM, respectively) at the output of the Viterbi convolutional decoder in order to guarantee a quasi-bit-error free transmission at the output of the Reed–Solomon block decoder ( $BER < 10^{-11}$ ). It is not easy to state what is the uncoded SER for symbol detection before the Viterbi decoder that produces the required BER performance after the decoding process. Indeed, it depends on the code rate (1/2, 2/3, 3/4, 5/6) that is imposed by puncturing, as well as on the residual correlation of the samples at the input of the decoder that is not completely eliminated by the finite-length interleavers. Moreover, a better performance can be obtained by using soft decision instead of hard decision decoding. Some simulation results obtained for the DVB-T convolutional code are shown in Fig. 4 by means of hard decision decoding in linear scenarios. The figure outlines how the quasi-error free condition translates in different requirements of uncoded BER performance depending on the channel

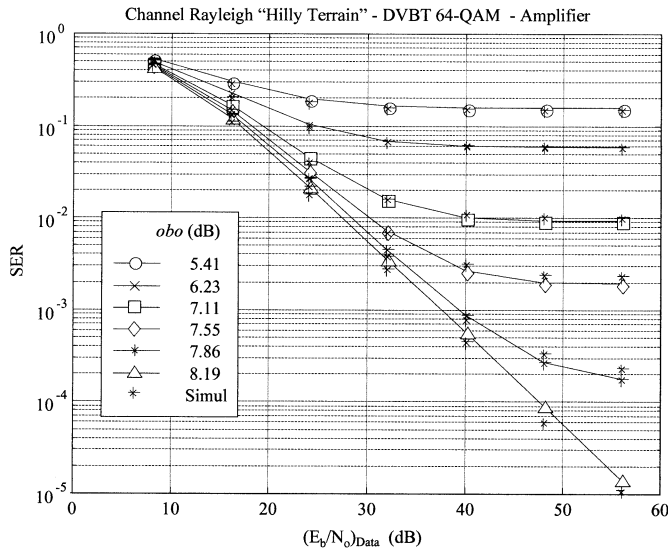


Fig. 3. Comparison of analytical and simulation results.

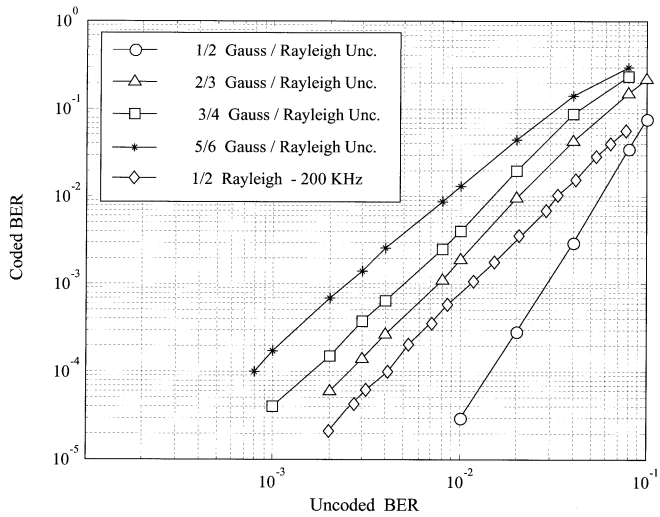
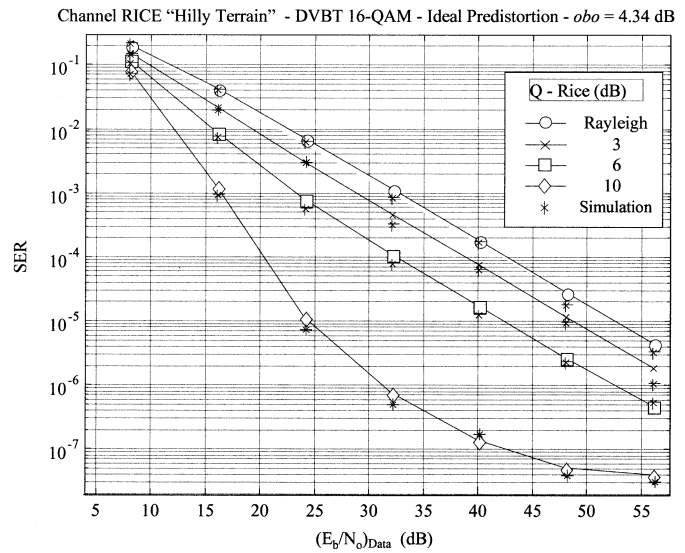


Fig. 4. Input-output BER for DVBT Viterbi hard decoder as a function of the code rate (1/2-2/3-3/4-5/6) and of the channel type (Gaussian—frequency uncorrelated; Rayleigh—frequency correlated Rayleigh).

coherence bandwidth and puncturing. The performance degradation due to the subcarriers correlation is highlighted for code rate equal to 1/2 and for a coherence bandwidth of 200 KHz, which causes a correlation of about 44 adjacent subcarriers for the subcarrier separation  $1/T_b \approx 4.46$  KHz in 2K-DVB-T. Anyway, it is possible to state that in most situations the required uncoded SER at the input of the Viterbi decoder lies between  $1 \cdot 10^{-3}$  and  $1 \cdot 10^{-2}$ .

As a consequence, the performance results of Figs. 3 and 5 have to be considered with particular attention to that SER range. Fig. 5(a), which shows the SER performance in the “hilly terrain” frequency-selective channel [16] characterized by a 10-dB power ratio  $Q$  between the direct and the scattered paths, suggests to choose, for the amplifier without predistortion, an  $obo$  of approximately 8.8 dB in order to avoid performance degradation. The optimum  $obo$  is usually defined as the one

that minimizes the so called “total degradation,” which is the sum of the  $obo$  and the excess ( $Eb/No$ ) that guarantees at this  $obo$  the same target SER performance with respect to the linear situation [24]. Indeed, an excessive  $obo$  reduction, which represents a power increase at the transmitter side, results in a power waste at the receiver side because of the higher signal power that is required to compensate for the increased nonlinear distortion noise. Fig. 5(b) shows the SER performance, in the same scenario, when the ideal amplifier predistortion is used and it suggests an optimum  $obo$  value of approximately 6.2 dB. The total degradation as a function of the  $obo$  is plotted in Fig. 6. This figure clearly shows that the gain obtained for Rice channels ( $Q = 10$  dB) by the predistortion technique is not limited to the 2.6 dB of reduced optimum  $obo$  but, by means of the total degradation concept, it also includes about 0.5 dB of lower SNR required at the receiver side to obtain the same SER performance. Moreover, Fig. 6 shows that the optimum  $obo$  depends on the channel statistic, suggesting a lower value for Rayleigh fading channels.

It should be pointed out that the choice of the optimum  $obo$  value for an OFDM system should also consider the signal spectral regrowth in the adjacent channels. Consequently, also the PSD as a function of the  $obo$  value should be evaluated by means of (9) [9].

Fig. 5(c) and (d) show the SER performance for two fixed  $obos$  as a function of the power ratio  $Q$  for selective Rice fading channels, spanning from a single direct path situation (AWGN when  $Q = \infty$ ) to the purely scattered situation (Rayleigh when  $Q = 0$ ).

An exhaustive analysis of all the possible combinations of modulation size  $M$ ,  $obo$  values and channel types for a DVB-T system is beyond the scope of the present work, which only uses DVB-T to illustrate the general results derived in this paper.

Fig. 5(c) also points out that the SER performance saturates to the same SER floor for a fixed  $obo$ . This is not surprising because this SER floor represents the SER performance when

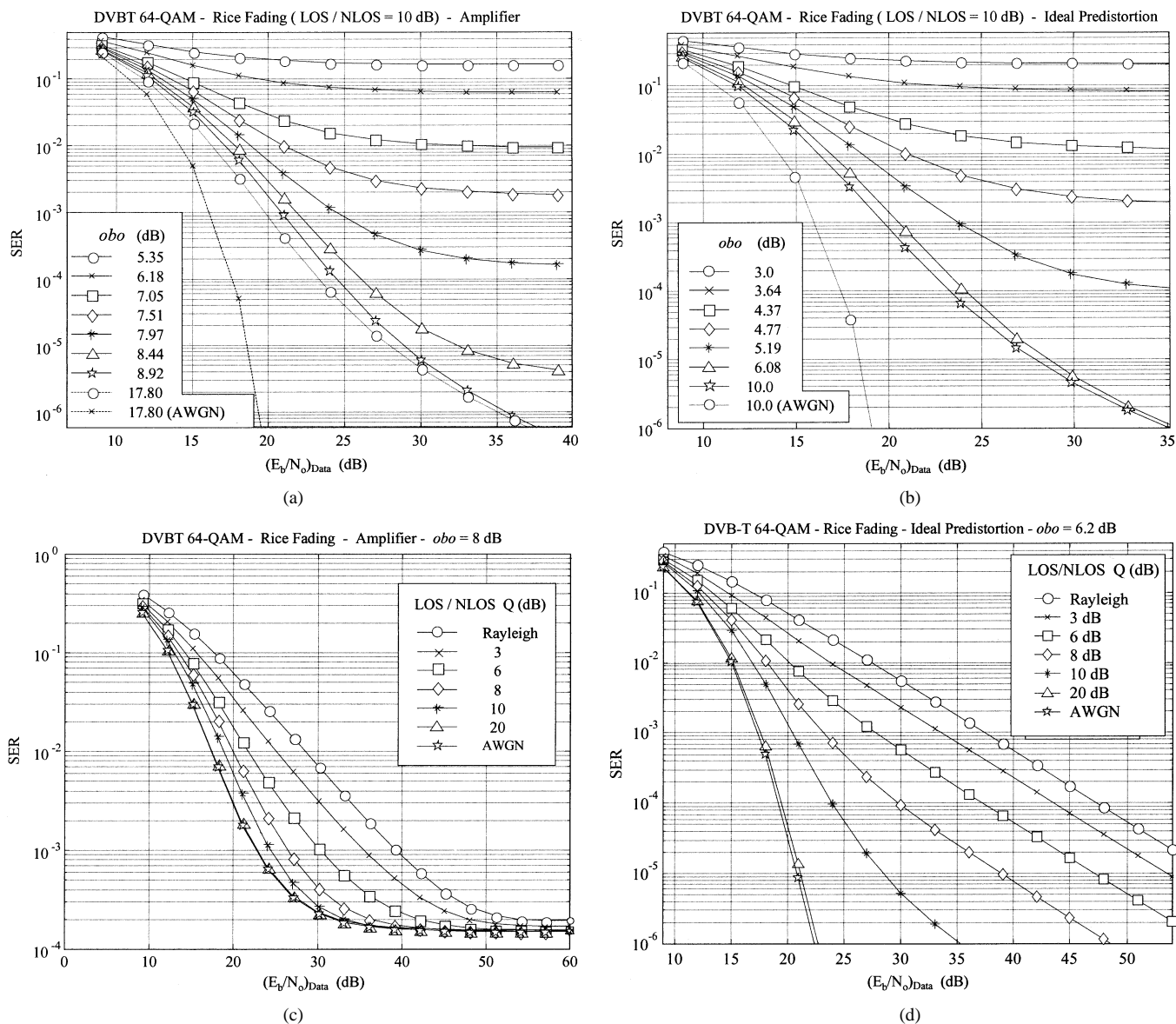


Fig. 5. Analytical performance results in different “hilly terrain” scenarios.

only the nonlinear distortion noise is present and the signal to thermal noise power ratio goes toward infinity. The nonlinear distortion noise does not depend on the channel. It is generated by the transmitter and faded by the channel in the same way as the useful signal. Consequently, the residual SER performance, in the absence of thermal noise, is the same for any channel that has been perfectly equalized. This fact is also useful when interpreting the analytical results obtained by numerical integration of (25) or (26). The numerical results obtained by exploiting the integration techniques of a widely known analytical tool [25] showed that expression (25) can sometimes introduce an approximation error that overestimates the real SER performance, acting as a numerical error floor on the SER performance. On the contrary, expression (26), which is generally characterized by a lower convergence speed, has a lower sensitivity to the numerical integral approximations and only exhibits some divergence problems for extremely high SNRs where the SER curves have generally already reached the nonlinear noise floor. An interesting point is the fact that the two algorithms

seem to be complementary, since where one fails the other one does not.

### V. CONCLUSION

We have derived the analytical computation of the uncoded SER performance for an OFDM system in nonlinear frequency-selective fading channels, thus generalizing the approach proposed in [9] for AWGN channels. The computer simulations conducted on a DVB-T system affected by frequency-selective fading channels compliant with the COST 207 proposal [16] have validated the proposed analytical approach. The approach allows predicting, with a dramatically reduced computation time, the uncoded system performance of an OFDM system in a realistic scenario impaired by a nonlinear distorting amplifier (even predistorted) and by frequency-selective fading channels, if perfect channel equalization is performed at the receiver.

The proposed approach can also be extended to compute the performance of real equalizers that estimate the channels. This,

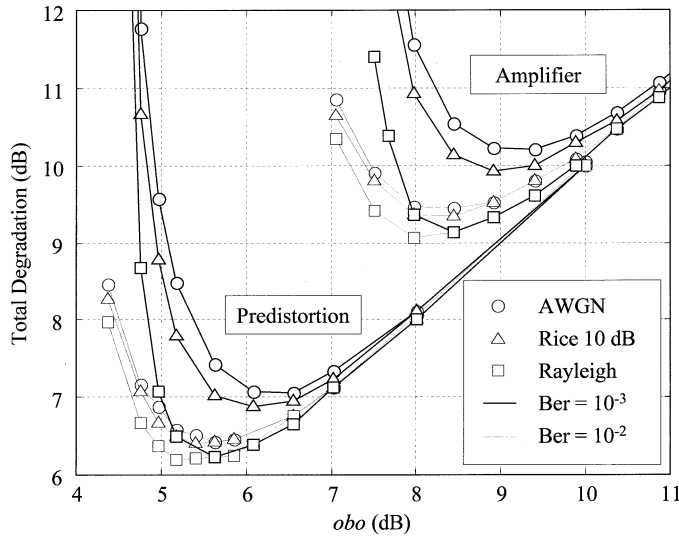


Fig. 6. Total degradation—DVBT 64-QAM.

TABLE II  
AMPLIFIER AM/AM AND AM/PM PARAMETERS

$m_o$	A = 1		Rmax = 3.5	
	$\text{Re}\{\beta_{m_o}\}$	$\text{Im}\{\beta_{m_o}\}$	$\text{Re}\{\beta_{m_o}\}$	$\text{Im}\{\beta_{m_o}\}$
1	1,66358406169717e+0	-9,56779304600097e-1	4,76342854300008e-2	2,67471791281399e-1
2	4,69785260752539e-1	4,76342854300008e-2	2,67471791281399e-1	1,56971628767209e-2
3	7,03924883468850e-2	2,67471791281399e-1	1,56971628767209e-2	-1,10981758342171e-1
4	-5,87943811793691e-2	1,56971628767209e-2	-1,10981758342171e-1	5,79037035641385e-2
5	-4,87673778456259e-2	-1,10981758342171e-1	5,79037035641385e-2	-3,43971630547126e-2
6	3,89877120603082e-2	5,79037035641385e-2	-3,43971630547126e-2	-5,28173986190222e-3
7	-3,36287740262672e-2	-5,28173986190222e-3	-5,28173986190222e-3	-4,13323082801559e-3
8	1,59554610608208e-2	-5,28173986190222e-3	-4,13323082801559e-3	3,43989816659608e-2
9	2,34981565219320e-2	-4,13323082801559e-3	3,43989816659608e-2	8,31848498525728e-3
10	-8,16688140613843e-3	3,43989816659608e-2	8,31848498525728e-3	-3,85377705226550e-2
11	-2,69062285577859e-2	8,31848498525728e-3	-3,85377705226550e-2	1,58473245288442e-2
12	1,39920227906391e-2	-3,85377705226550e-2	1,58473245288442e-2	
13	6,30296132414095e-3	1,58473245288442e-2		

as well as the extension of the analytical approach to take other error sources like frequency synchronization errors into account, could be the subject of future work.

## APPENDIX I

## PDF OF THE SNR IN NONLINEAR ENVIRONMENT

The SNR in the nonlinear fading environment is expressed by (23), which is rewritten here as  $(\chi_{\text{TOT}})_n = g(\chi)$ . It is well known that the pdf of the random variable  $(\chi_{\text{TOT}})_n$  can be obtained by

$$\begin{aligned}
 p_{X_{\text{TOT}}}(\chi_{\text{TOT}}) &= \frac{p_X(\chi_1)}{|g'(\chi_1)|} \\
 \chi_1 &= g^{-1}(\chi_{\text{TOT}}) \\
 &= \frac{1}{|\alpha|^2} \frac{\chi_{\text{NL}} \chi_{\text{TOT}}}{\chi_{\text{NL}} - \chi_{\text{TOT}}} \quad (\text{A.1})
 \end{aligned}$$

where  $p_X(\chi)$  is the pdf of the SNR in the linear case. It is easy to show that  $\chi_{\text{TOT}}$  is distributed as expressed by

$$\begin{aligned}
 p_{X_{\text{TOT}}}(\chi_{\text{TOT}}) &= \frac{1}{|\alpha|^2 \chi_o} \left[ \frac{\chi_{\text{NL}}}{\chi_{\text{NL}} - \chi_{\text{TOT}}} \right]^2 \\
 &\quad \cdot \exp\left(-\frac{\chi_{\text{NL}}}{\chi_{\text{NL}} - \chi_{\text{TOT}}} \cdot \frac{\chi_{\text{TOT}}}{|\alpha|^2 \chi_o}\right) \\
 \chi_{\text{TOT}} &\in [0, \chi_{\text{NL}}] \quad (\text{A.2})
 \end{aligned}$$

if  $\chi$  is distributed as an exponential RV, while  $\chi_{\text{TOT}}$  is distributed as

$$\begin{aligned}
 p_{X_{\text{TOT}}}(\chi_{\text{TOT}}) &= \frac{1+Q^2}{|\alpha|^2 \chi_o} \left[ \frac{\chi_{\text{NL}}}{\chi_{\text{NL}} - \chi_{\text{TOT}}} \right]^2 \exp(-Q^2) \\
 &\quad \cdot \exp\left(-\frac{\chi_{\text{NL}}}{\chi_{\text{NL}} - \chi_{\text{TOT}}} \cdot \frac{(1+Q^2)\chi_{\text{TOT}}}{|\alpha|^2 \chi_o}\right) \\
 &\quad \cdot I_0\left(2Q \sqrt{\frac{\chi_{\text{NL}}}{\chi_{\text{NL}} - \chi_{\text{TOT}}} \cdot \frac{(1+Q^2)\chi_{\text{TOT}}}{|\alpha|^2 \chi_o}}\right), \chi_{\text{TOT}} \in [0, \chi_{\text{NL}}] \quad (\text{A.3})
 \end{aligned}$$

if  $\chi$  is distributed as a noncentral chi-squared RV.

## APPENDIX II

## AM-AM AND AM-PM PARAMETERS

Table II reports the parameters  $A$  and  $R_{\text{max}}$ , as well as the complex coefficients  $\beta_{m_o}$  of (11) used to represent the amplifier AM/M and AM/PM distorting curves of Fig. 2.

## REFERENCES

- [1] "ETSI," Radio broadcast systems; Digital audio broadcasting (DAB) to mobile, portable, and fixed receivers, ETS 300 401, May 1997.
- [2] "ETSI," Digital video broadcasting (DVB-T); Framing structure, channel coding, and modulation for digital terrestrial television, ETS 300 744, Dec. 2001.
- [3] "ETSI," Broadband radio access network (BRAN): HYPERLAN Type 2 functional specification Part 1—Physical layer, DTS/BRAN 030 003-1, June 1999.
- [4] Z. Wang and G. B. Giannakis, "Wireless multicarrier communications," *IEEE Signal Processing Mag.*, pp. 29–48, May 2000.
- [5] A. Ruiz, J. M. Cioffi, and S. Kasturia, "Discrete multiple tone modulation with coset coding for the spectrally shaped channel," *IEEE Trans. Commun.*, vol. 40, pp. 1012–1029, June 1992.
- [6] L. J. Cimini Jr., "Analysis and simulation of a digital mobile channel using orthogonal frequency division multiplexing," *IEEE Trans. Commun.*, vol. 33, pp. 665–675, July 1985.
- [7] J. Minkoff, "The role of AM-to-PM conversion in memoryless nonlinear systems," *IEEE Trans. Commun.*, vol. COM-33, pp. 139–143, Feb. 1985.
- [8] A. Papoulis, *Probability, Random Variables and Stochastic Process*, 3rd ed. New York: McGraw-Hill, 1991.
- [9] P. Banelli and S. Cacopardi, "Theoretical analysis and performance of OFDM signals in nonlinear AWGN channels," *IEEE Trans. Commun.*, vol. 48, pp. 430–441, Mar. 2000.
- [10] D. Dardari, V. Tralli, and A. Vaccari, "A theoretical characterization of nonlinear distortion effects in OFDM systems," *IEEE Trans. Commun.*, vol. 48, pp. 1755–1764, Oct. 2000.
- [11] E. Costa, M. Midrio, and S. Pupolin, "Impact of amplifier nonlinearities on OFDM transmission system performance," *IEEE Commun. Lett.*, vol. 3, pp. 37–39, Feb. 1999.
- [12] Ziemer and Peterson, *Introduction to Digital Communication*, 2nd ed. Englewood Cliffs, NJ: Prentice-Hall, 2001.
- [13] N. M. Blachman, "Bandpass nonlinearities," *IEEE Trans. Inform. Theory*, vol. 10, pp. 162–164, Apr. 1964.
- [14] A. R. Kaye, D. A. George, and M. J. Eric, "Analysis and compensation of bandpass nonlinearities for communications," *IEEE Trans. Commun.*, vol. COM-20, pp. 965–972, Oct. 1972.

- [15] J. G. Proakis, *Digital Communications*, 3rd ed. New York: McGraw-Hill, 1995.
- [16] "Digital mobile communications-COST 207," Office for Official Publications of the European Communities, Luxembourg, 1989.
- [17] M. S. Alouini and A. J. Goldsmith, "A unified approach for calculating error rates of linearly modulated signals over generalized fading channels," *IEEE Trans. Commun.*, vol. 47, pp. 1324–1334, Sept. 1999.
- [18] H. Sari, G. Karam, and I. Jeanclaude, "An analysis of orthogonal frequency-division multiplexing for mobile radio applications," in *Proc. IEEE Vehicular Technology Conf. '94*, vol. 3, Stockholm, Sweden, June 1994, pp. 1635–1639.
- [19] G. Santella and F. Mazzenga, "A model for performance evaluation in M-QAM-OFDM schemes in presence of nonlinear distortion," in *Proc. IEEE Vehicular Technology Conf. '95*, vol. 2, Chicago, IL, July 1995, pp. 830–834.
- [20] E. Biglieri, J. Proakis, and S. Shamai, "Fading channels: Information-theoretic and communications aspects," *IEEE Trans. Inform. Theory*, vol. 44, pp. 2619–2692, Oct. 1998.
- [21] T. May, H. Rohling, and V. Engels, "Performance analysis of Viterbi decoding for 64-DAPSK and 64-QAM modulated OFDM signals," *IEEE Trans. Commun.*, vol. 46, pp. 182–190, Feb. 1998.
- [22] M. Sandell, S. K. Wilson, and P. O. Börjesson, "Performance analysis of coded OFDM on fading channels with nonideal interleaving and channel knowledge," in *Proc. IEEE Vehicular Technology Conf. '97*, vol. 3, Phoenix, AZ, May 1997, pp. 1380–1384.
- [23] A. Chini, M. S. El-Tanany, and S. A. Mahmoud, "On the performance of a coded MCM over multipath Rayleigh fading channels," in *Proc. IEEE ICC 95*, vol. 3, Seattle, WA, June 1995, pp. 1689–1694.
- [24] G. Karam and H. Sari, "Data predistortion techniques using intersymbol interpolation," *IEEE Trans. Commun.*, vol. 38, no. 10, pp. 1716–1723, Oct. 1990.
- [25] "The language of technical computing," The MathWorks Inc., Natick, MA, MATLAB 5.3- Rel.11, 1999.



**Paolo Banelli** (S'90–M'99) was born in Perugia, Italy, on May 19, 1968. He received the Laurea degree in electronics engineering and the Ph.D. degree in telecommunications both from the University of Perugia, Perugia, Italy, in 1993 and 1998, respectively.

Since 1998, he has been an Assistant Professor with the Department of Electronic and Information Engineering (DIEI), University of Perugia. In 2001, he joined as a Visiting Researcher the SpinComm Group at the Electronic and Computer Engineering Department, University of Minnesota, Minneapolis. His research interests include nonlinear distortions, broadcasting, multiuser detection, and block-transmission techniques for wireless communications.

Dr. Banelli is a Member of the Communications Society.